

## Self-Templated Nucleation in Peptide and Protein Aggregation

Stefan Auer,<sup>1,\*</sup> Christopher M. Dobson,<sup>2</sup> Michele Vendruscolo,<sup>2,†</sup> and Amos Maritan<sup>3</sup>

<sup>1</sup>*Centre for Self Organising Molecular Systems, University of Leeds, Leeds LS2 9JT, United Kingdom*

<sup>2</sup>*Department of Chemistry, University of Cambridge, Lensfield Road, Cambridge CB2 1EW, United Kingdom*

<sup>3</sup>*Dipartimento di Fisica, Università di Padova, INFN and CNISM, Via Marzolo 8, 35131 Padova, Italy*

(Received 18 August 2008; published 17 December 2008)

Peptides and proteins exhibit a common tendency to assemble into highly ordered fibrillar aggregates, whose formation proceeds in a nucleation-dependent manner that is often preceded by the formation of oligomeric assemblies. This process has received much attention because disordered oligomeric aggregates have been associated with neurodegenerative disorders such as Alzheimer's and Parkinson's disease. Here we describe a self-templated nucleation mechanism that determines the transition between the initial condensation of polypeptide chains into disordered assemblies and their reordering into fibrillar structures. The results that we present show that at the molecular level this transition is due to the ability of polypeptide chains to reorder within oligomers into fibrillar assemblies whose surfaces act as templates that stabilize the disordered assemblies.

DOI: 10.1103/PhysRevLett.101.258101

PACS numbers: 87.15.A–, 87.14.E–

There are two fundamental questions that one can ask about the general phenomenon of the formation of ordered structures by atoms and molecules. The first concerns the type of assembly that the given particles can form, and the second the kinetic paths that the particles follow in order to reach a stable structure. The answer to the first question, at least in the cases when the particles are rigid, is that in nature there exists only a small number of possible crystal structures, corresponding to the 230 crystallographic space groups [1]. The extraordinary power of this result, which is based on symmetry and geometry arguments, is that the answer is independent of the specific particles and of their mutual interactions. The properties of the specific particles merely determine which type of crystal structure is the most stable. The answer to the second question is generally more difficult, although it is likely to involve a nucleation and growth mechanism [2]. In this mechanism the atoms first need to come together to form a critical nucleus (the nucleation phase), before they can grow (the elongation phase). The probability  $P_c$  that a spontaneous fluctuation will result in the formation of a critical nucleus depends exponentially on the free energy  $\Delta F_c$  required to form such a nucleus:  $P_c = \exp(-\Delta F_c/kT)$ , where  $T$  is the absolute temperature and  $k$  is the Boltzmann constant. In atomic systems the activation barriers are usually very high, and the probability of observing nuclei is very small; even when nuclei form, their lifetime is fleetingly short, so that up to now there has been no definitive experimental observation of critical nuclei in atomic systems, and computer simulations have become a major tool for investigating this phenomenon [3].

An additional problem arises when the particles forming the ordered structures are not rigid, but flexible, as is the case for peptides and proteins. Individual molecules of this type often have an intrinsic tendency to fold into ordered structural patterns, which may either favor or hinder their

intermolecular assembly process. This problem constitutes an entirely new chapter in the study of molecular ordering that has very great significance for biology and biotechnology. Indeed, biomolecules such as DNA and proteins have recurrent structural motifs such as  $\alpha$  helices and  $\beta$  sheets [4], and a wide range of different proteins can assemble into highly ordered fibrillar aggregates [5]. Although the amino acid sequences of these proteins are often unrelated, the structures of the resulting amyloid fibrils show a common characteristic cross- $\beta$  structure in which the main axis of individual molecules runs orthogonal to the direction of the filaments. It has thus been suggested that the inherent ability to form fibrillar assemblies is a feature common to polypeptide chains [6].

In order to explain why this process takes place despite the remarkable resistance of native states of proteins to aggregation, a “nucleated conformational conversion” mechanism has been proposed in which the formation of highly dynamic oligomeric assemblies facilitates the further conversion of polypeptide chains into ordered fibrillar structures [7]. Evidence in favor of this mechanism has been provided through experimental [5,8,9] and theoretical studies [10–15]. In this Letter we exploit the ability of computer simulations to provide a description of molecular processes at very high resolution—an ability that has proved invaluable in defining nucleation processes in atomic and colloidal systems [3,16]. In the case of polypeptide chains, we have recently shown that it is possible to follow the aggregation process for times long enough to include both the initial condensation into disordered oligomeric assemblies and their subsequent reorganization into fibrillar structures [15,17], and that the nucleated conformational conversion mechanism can also be described as a “condensation-reordering” mechanism (Fig. 1).

In this Letter we further study the condensation-ordering mechanism by investigating the self-templated nucleation

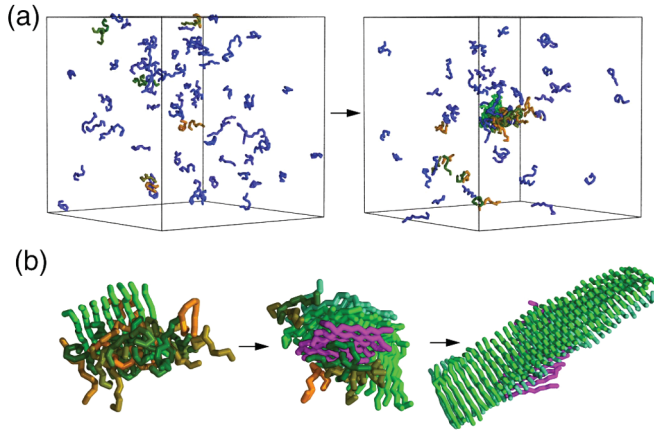


FIG. 1 (color). Condensation-reordering mechanism at  $c = 12.5$  mM and  $T^* = 0.66$  above the folding temperature. Peptides that do not form interchain hydrogen bonds are shown in blue, those forming interchain hydrogen bonds are assigned a random color. Peptides within the same  $\beta$  sheet are assigned the same color. (a) Initially, at  $t \leq 1000$ , the peptides are in a monomeric state (left panel). The progress variable  $t$  represents the number of Monte Carlo moves performed in the simulation; one unit of  $t$  is a block of  $10^5$  Monte Carlo moves. As the simulation progresses, a hydrophobic collapse causes the formation of a small disordered oligomer ( $t = 15\,000$ , right panel). (b) Enlarged view of a disordered oligomer which subsequently orders into a protofilament structure:  $t = 15\,000$  (left),  $t = 19\,000$  (middle),  $t = 30\,000$  (right).

mechanism that determines the coupling between the assembly of polypeptide chains into disordered oligomers and the transformation into highly ordered cross- $\beta$  structures. A template model by which misfolded prions induce the conversion of nearby native prions to the misfolded state has already been proposed [18], and simulated for SH3 [19] and cc $\beta$  [20]. In particular, in the latter case it was shown that  $\beta$  sheets with exposed hydrophobic surfaces and unsaturated hydrogen bonds accelerate the conversion of native  $\alpha$  helices into  $\beta$  sheets.

The computational strategy that we follow is based on the attempt to reproduce simultaneously two common aspects of proteins, their ability to form secondary structural motifs [21], and their propensity to form ordered fibrillar aggregates [5]. Recently it has been shown that motifs such as  $\alpha$  helices,  $\beta$  sheets and cross- $\beta$  structures are natural forms of a marginally compact phase of matter characteristic of flexible polymers [22,23]. The description of proteins in terms of flexible tubes captures in a simple way the primary symmetry of chain molecules. In this approach, a polypeptide chain is represented by a chain of finite thickness, which approximately envelops the backbone atoms. The hydrophobic effects due to the solvent are considered by a pairwise additive interaction between different  $C_\alpha$  atoms, which are explicitly represented in the chain, with an energy  $e_{HP}$ , when they are close. The sequence-independent definition of hydrogen bonding is obtained by an analysis of the geometric prop-

erties of hydrogen bonds from the Protein Data Bank, and assigned an energy  $e_{HB}$ . Steric constraints due to side chains are imposed by local bending stiffness with energy  $e_S$ ; for a detailed description of the model see [17,24].

Based on the hypothesis that the formation of amyloid fibrils is a common feature of all polypeptide chains, which depends mainly on the generic properties of their backbone [25,26], we investigated the behavior of a representative model system consisting of 80 weakly hydrophobic 12-residue homopolymers. Systems of homopolymers [27] have been shown experimentally to form amyloid assemblies. In all our simulations the energy of a hydrogen bond was set to  $e_{HB} = -3kT_0$ , a value close to experiment (1.5 kcal/mol at room temperature [28]). Here  $kT_0$  is a reference thermal energy and the reduced temperature is  $T^* = T/T_0$ . The hydrophobic and stiffness energy were set to  $e_{HP} = -0.15kT_0$  and  $e_S = 0.9kT_0$ , respectively. The ratio  $e_{HB}/e_{HP} = 20$  is such that these interactions provide similar overall contributions to the potential energy of the oligomer [15]. With this choice of parameters the peptides form an  $\alpha$  helical native structure below the folding temperature  $T_f^* \sim 0.6$ , and a random coil structure above.

In order to illustrate the condensation-reordering transition (Fig. 1) we set the peptide concentration to  $c = 12.5$  mM and the reduced temperature to  $T^* = 0.66$ , to keep the lag time prior to aggregation very short. Lowering the concentration, while keeping the temperature constant, results in a dramatic increase in the lag time. At  $c = 1$  mM the peptides remain monomeric on the time scale that we have been able to follow, although the aggregated state is likely to be much more stable than the monomeric state. In this concentration regime ( $c = 1$  mM to  $c = 12.5$  mM) the monomeric state is metastable with respect to the aggregated state, and the aggregation of polypeptide chains follows a nucleation mechanism [29]. Under such conditions we calculated the nucleation barriers associated with the condensation-reordering transition.

A prerequisite for such a calculation is the ability to describe quantitatively the formation of small oligomeric assemblies. By using a standard cluster criterion, i.e., that any two peptides whose distances between their centers of mass is less than  $5 \text{ \AA}$  belong to the same oligomer, it is possible to define the oligomer size  $n$ , that corresponds to the number of peptides within the oligomer. At the same time it is possible to measure the  $\beta$ -sheet content of the oligomer. As the formation of  $\beta$  sheets is driven by interchain hydrogen bonding, we use  $m$ , the number of interchain hydrogen bonds formed within an oligomer, as a structural observable. In order to calculate the joint equilibrium probability  $P(n, m)$  for the formation of an oligomeric assembly consisting of  $n$  peptides with  $m$  interchain hydrogen bonds we performed biased Monte Carlo simulations [16,17] in the canonical ensemble using crankshaft, pivot, reptation, rotation, and translation moves. As a biasing potential we included an additional parabolic energy term,  $W = \alpha(m - m_0)^2$ , in the energy function, where  $\alpha$

and  $m_0$  are parameters, that can be used to control the range of  $m$  values sampled in the simulation. The calculation of  $P(n, m)$  was split into 28 independent simulations for different  $m_0$  values, and then recombined into one by a multihistogram technique. The corresponding nucleation free-energy landscape, apart from an additive constant, is given by  $F(n, m) = -kT^* \ln[P(n, m)]$ . A representative calculation of such a free-energy landscape obtained at  $c = 1.2$  mM and  $T^* = 0.51$  (i.e., below  $T_f^*$ ) is shown in Fig. 2(a). The succession of local minima in this landscape reveals the central result of this work—that the oligomer size  $n$  and the number of hydrogen bonds  $m$  in the states of minimal free energy for the oligomers are coupled. To clarify the nature of this coupling we analyzed the structure of the oligomers formed in the local minima of the free-energy landscape. As an example, we show in the inset of Fig. 2(a) that the oligomer corresponding to the minimum ( $n = 13, m = 68$ ) consists of  $n_\beta = 8$  peptides in a  $\beta$ -sheet conformation and  $n_\alpha = 5$  in a helical conformation. Here we define two peptides to be part of a  $\beta$  sheet if they form

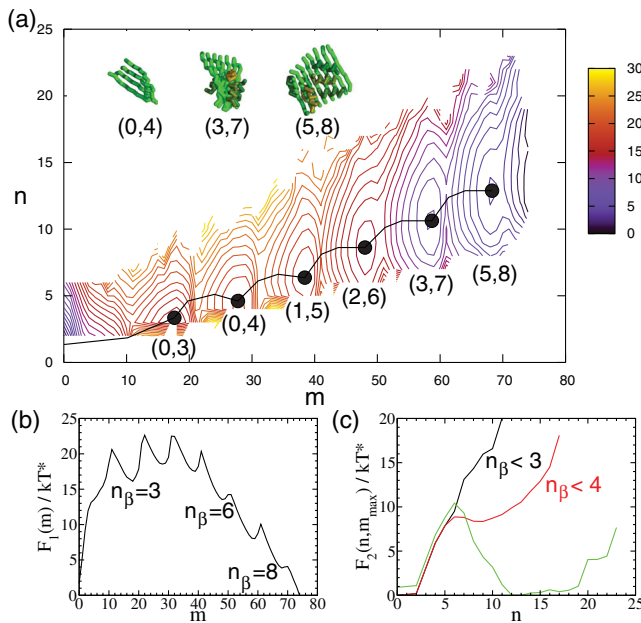


FIG. 2 (color). (a) Contour plot of the nucleation barrier  $F(n, m)$  calculated at a concentration  $c = 1.2$  mM and a reduced temperature  $T^* = 0.51$ ; the latter is below the folding temperature. The black circles indicate the minima on the free-energy surface, and the black line indicates a possible path that connects them. The labels  $(n_\alpha, n_\beta)$  of the minima describe the structures of the oligomers, where  $n_\alpha$  and  $n_\beta$  are, respectively, the number of peptides in  $\alpha$ -helical and  $\beta$ -strand structure, and  $n = n_\alpha + n_\beta$ . In the inset we show snapshots of the oligomers associated with the minima. (b) Nucleation barrier for  $\beta$ -sheet formation,  $F_1(m)$ , as a function of the number of interchain hydrogen bonds  $m$  that are formed within the oligomer. (c) Nucleation barrier  $F_2(n, m_{\max})$  for the formation of an oligomer of size  $n$  that can at most form  $m_{\max}$  interchain hydrogen bonds:  $m_{\max} = 10$  ( $n_\beta < 3$ ) (black line),  $m_{\max} = 20$  ( $n_\beta < 4$ ) (red line), all  $m$  values included (green line).

more than four interchain hydrogen bonds with each other. Since the peptides within the oligomer are either in an  $\alpha$ -helical or  $\beta$ -strand conformation,  $n = n_\alpha + n_\beta$ , we label each minimum by the pair  $(n_\alpha, n_\beta)$ . Typical configurations of other oligomers are also shown in the inset of Fig. 2(a). We further analyze this coupling in Fig. 3, where we plot, for the states corresponding to the minima of the free energy, the number  $n_\alpha$  of peptides in an  $\alpha$ -helical conformation within an oligomer as a function of the number  $n_\beta$  of peptides in a  $\beta$ -sheet conformation. The essentially linear relationship indicates that the probability of oligomeric assemblies increases with the size of the ordered  $\beta$ -sheet structures.

To reveal the molecular basis of this coupling, we have analyzed the nucleation barrier for  $\beta$ -sheet formation independently of the number of peptides in an  $\alpha$ -helical conformation. The average over  $n$  is achieved by the marginalization of  $P(n, m)$  with respect to  $n$ , and its corresponding free-energy profile is  $F_1(m) = -kT^* \ln[\sum_n P(n, m)]$ . The calculations indicate that  $F_1(m)$  is comprised of a series of component barriers, each separated by  $\Delta m = 10$  [Fig. 2(b)]. Since in the case considered here each pair of peptides in a  $\beta$ -sheet conformation can form at most ten interchain hydrogen bonds with each other, each maximum of  $F_1(m)$  corresponds to the addition of a new peptide to the existing  $\beta$ -sheet structure within the oligomer. After the first few interchain hydrogen bonds are formed, the free energy decreases until an optimal number of hydrogen bonds is formed, corresponding to a local minimum. The elongation barrier for  $\beta$ -sheet nucleation

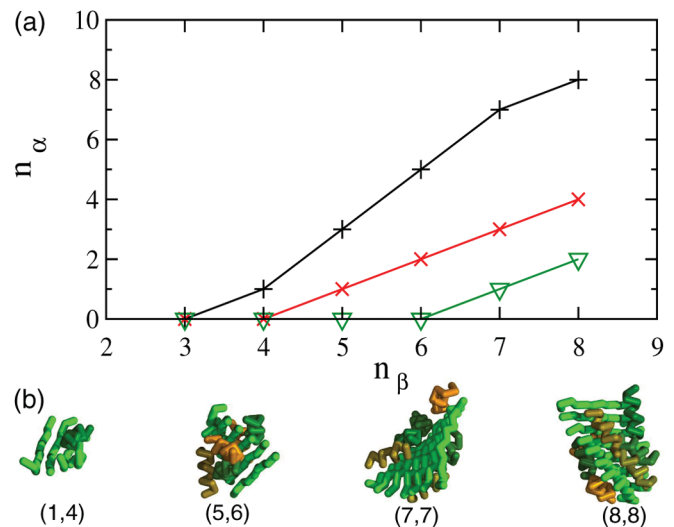


FIG. 3 (color). Correlations for the successive minima in the free-energy landscape [such as shown in Fig. 2(a)] between the number  $n_\alpha$  of peptides in an  $\alpha$ -helical conformation and the number  $n_\beta$  of peptides in a  $\beta$ -sheet conformation. (a) Correlations obtained at  $T^* = 0.51$  and  $c = 0.64$  mM (green line),  $c = 1.2$  mM (red line) and  $c = 2.9$  mM (black line). (b) Typical configurations of the oligomers associated with the minima obtained at  $T^* = 0.51$  and  $c = 2.9$  mM [black line in (a)].

corresponds to the free energy needed to transform a peptide from its  $\alpha$ -helical conformation to the extended structure it has in its  $\beta$ -sheet conformation. The elongation barrier is a quantitative measure for the aggregation propensities of proteins, and can be measured experimentally [26]. In our calculation a dimer formed by two  $\beta$  strands is always unstable and disassembles soon after it forms; the critical size of the  $\beta$  sheet is a tetramer, at least in the range of concentrations and temperatures that we explored.

Next we investigated how the nucleation barrier for the formation of an oligomer depends on its internal structure, i.e., if a  $\beta$  sheet is present or not. The structural average over  $m$  is obtained by resorting to the marginal distribution function  $P(n, m \leq m_{\max}) \equiv \sum_{m=0}^{m_{\max}} P(n, m)$  and the corresponding free-energy profile is given by  $F_2(n, m_{\max}) = -kT^* \ln P(n, m \leq m_{\max})$ . Here  $F_2(n, m_{\max})$  is the nucleation barrier for forming an oligomer of  $n$  peptides, with at most  $m_{\max}$  interchain hydrogen bonds. This upper limit to the number of interchain hydrogen bonds is introduced in the projection operation with the goal of unveiling the role of the  $\beta$ -sheet structure formed within the oligomer in the dynamical evolution of the aggregation process. If we do not allow the formation of  $\beta$  sheets consisting of more than two peptides, by imposing  $m_{\max} = 10$ , the free energy for the formation of an oligomer increases monotonically [Fig. 2(c), black line]. If we allow the formation of  $\beta$  sheets consisting of up to three peptides, by relaxing the constrain to  $m_{\max} = 20$ , we observe that after an initial increase, for  $n < 5$ , a local minimum is present at  $n_{\min} = 10$  [Fig. 2(c), red line]. Then, for  $n > n_{\min}$ , the free energy increases again because  $\alpha$ -helical oligomers are not stable under these conditions. The existence of a local minimum of this type has never been observed in atomic or molecular systems where the nucleation barrier increases monotonically until a critical size, and then decreases monotonically for larger sizes [2]. Inclusion of all  $m$  values sampled during simulation in the summation relieves all constrains on the number of  $\beta$  sheets formed within the oligomer and we find that the position of the local minimum of  $F_2$  moves to a larger value  $n_{\min} \sim 15$  [Fig. 2(c), green line].

These results provide a molecular description of the origin of the coupling between the nucleation events leading to the formation of fibrillar structures. The ability of polypeptide chains to reorganize within oligomers into a fibrillar structure stabilizes oligomeric assemblies since the surface of a growing  $\beta$  sheet acts as a substrate for the attachment of other  $\alpha$ -helical peptides. This self-templated nucleation mechanism is also found for the aggregation process above the folding temperature (see Fig. 1), but the associated nucleation barriers are smaller. In systems where proteins form complex structural motifs in the monomeric phase, the activation barriers for aggregation into  $\beta$  sheets are likely to be higher, and the templating effect in the nucleation mechanism might be more pronounced. The results of this study therefore indicate that a better understanding of this mechanism should lead to an

increasing ability to modulate the growth of peptide and protein aggregates, and could play an important role in the development of therapies for conditions such as Alzheimer's and Parkinson's disease [30].

We thank A. Aggeli, E. Paci, P. Olmsted, and J.R. Banavar for illuminating discussions.

\*Corresponding author: s.auer@leeds.ac.uk

†Corresponding author: mv245@cam.ac.uk

- [1] J. F. Cornwell, *Group Theory in Physics* (Academic Press, London, UK, 1984), Vol. 1.
- [2] K. F. Kelton, *Solid State Physics* (Academic Press, San Diego, 1991).
- [3] R. P. Sear, *J. Phys. Condens. Matter* **19**, 033101 (2007).
- [4] B. Alberts *et al.*, *Molecular Biology of the Cell* (Garland Publishing, New York, 2002).
- [5] F. Chiti and C. M. Dobson, *Annu. Rev. Biochem.* **75**, 333 (2006).
- [6] C. M. Dobson, *Nature (London)* **426**, 884 (2003).
- [7] T. R. Serio *et al.*, *Science* **289**, 1317 (2000).
- [8] M. Tanaka *et al.*, *Nature (London)* **442**, 585 (2006).
- [9] A. Lomakin *et al.*, *Proc. Natl. Acad. Sci. U.S.A.* **93**, 1125 (1996).
- [10] B. Urbanc *et al.*, *Proc. Natl. Acad. Sci. U.S.A.* **101**, 17345 (2004).
- [11] H. D. Nguyen and C. K. Hall, *Proc. Natl. Acad. Sci. U.S.A.* **101**, 16180 (2004).
- [12] B. Ma and R. Nussinov, *Curr. Opin. Chem. Biol.* **10**, 445 (2006).
- [13] R. D. Hills and C. L. Brooks, *J. Mol. Biol.* **368**, 894 (2007).
- [14] R. Pellarin and A. Caflisch, *J. Mol. Biol.* **360**, 882 (2006).
- [15] S. Auer *et al.*, *PLoS Comp. Biol.* **4**, e1000222 (2008).
- [16] S. Auer and D. Frenkel, *Nature (London)* **409**, 1020 (2001).
- [17] S. Auer, C. M. Dobson, and M. Vendruscolo, *HFSP J.* **1**, 137 (2007).
- [18] S. B. Prusiner, *Proc. Natl. Acad. Sci. U.S.A.* **95**, 13363 (1998).
- [19] F. Ding *et al.*, *J. Mol. Biol.* **324**, 851 (2002).
- [20] F. Ding, J. J. LaRocque, and N. V. Dokholyan, *J. Biol. Chem.* **280**, 40235 (2005).
- [21] L. Pauling, R. B. Corey, and H. R. Branson, *Proc. Natl. Acad. Sci. U.S.A.* **37**, 205 (1951).
- [22] J. R. Banavar *et al.*, *Phys. Rev. E* **70**, 041905 (2004).
- [23] J. R. Banavar and A. Maritan, *Annu. Rev. Biophys. Biomol. Struct.* **36**, 261 (2007).
- [24] T. X. Hoang *et al.*, *Proc. Natl. Acad. Sci. U.S.A.* **101**, 7960 (2004).
- [25] C. M. Dobson, *Trends Biochem. Sci.* **24**, 329 (1999).
- [26] T. P. J. Knowles *et al.*, *Proc. Natl. Acad. Sci. U.S.A.* **104**, 10016 (2007).
- [27] A. Aggeli *et al.*, *Proc. Natl. Acad. Sci. U.S.A.* **98**, 11857 (2001).
- [28] A. R. Fersht *et al.*, *Nature (London)* **314**, 235 (1985).
- [29] J. T. Jarrett and P. T. Lansbury, *Cell* **73**, 1055 (1993).
- [30] C. Haass and D. J. Selkoe, *Nat. Rev. Mol. Cell Biol.* **8**, 101 (2007).